JCI The Journal of Clinical Investigation

Fragile TIM-4–expressing tissue resident macrophages are migratory and immunoregulatory

Thomas B. Thornley, … , Vijay K. Kuchroo, Terry B. Strom

J Clin Invest. 2014;124(8):3443-3454. https://doi.org/10.1172/JCI73527.

Research Article **Immunology**

Macrophages characterized as M2 and M2-like regulate immune responses associated with immune suppression and healing; however, the relationship of this macrophage subset to $CD169^+$ tissue-resident macrophages and their contribution to shaping alloimmune responses is unknown. Here we identified a population of M2-like tissue-resident macrophages that express high levels of the phosphatidylserine receptor TIM-4 and CD169 ($TIM\text{-}4^{hi}CD169^+$). Labeling and tracking of $TIM\text{-}4^{hi}CD169^+$ macrophages in mice revealed that this population is a major subset of tissue-resident macrophages, homes to draining LNs following oxidative stress, exhibits an immunoregulatory and hypostimulatory phenotype that is maintained after migration to secondary lymphoid organs, favors preferential induction of antigen-stimulated Tregs, and is highly susceptible to apoptosis. Moreover, $CD169^+$ tissue-resident macrophages were resistant to oxidative stress–induced apoptosis in mice lacking TIM-4. Compared with heart allografts from WT mice, *Tim4*$^{-/-}$ heart allografts survived much longer and were more easily tolerized by non-immunosuppressed recipients. Furthermore, *Tim4*$^{-/-}$ allograft survival was associated with the infiltration of Tregs into the graft. Together, our data provide evidence that M2-like $TIM\text{-}4^{hi}CD169^+$ tissue-resident macrophages are immunoregulatory and promote engraftment of cardiac allografts, but their influence is diminished by TIM-4–dependent programmed cell death.

Fragile TIM-4–expressing tissue resident macrophages are migratory and immunoregulatory

Thomas B. Thornley,[1] Zemin Fang,[1,2] Savithri Balasubramanian,[1] Rafael A. Larocca,[1] Weihua Gong,[1] Shipra Gupta,[1] Eva Csizmadia,[1] Nicolas Degauque,[1,3] Beom Seok Kim,[1,4] Maria Koulmanda,[1] Vijay K. Kuchroo,[5] and Terry B. Strom[1]

[1]Department of Medicine, Harvard Medical School, Transplant Institute at Beth Israel Deaconess Medical Center, Boston, Massachusetts, USA. [2]Department of Cardiothoracic Surgery, Tongji Hospital, Tongji Medical College, Huazhong University of Science and Technology, Wuhan, Hubei, China. [3]Institut National de la Santé et de la Recherche Médicale and Institut de Transplantation Urologie Néphrologie, Nantes, France. [4]Department of Internal Medicine, Yonsei University College of Medicine, Seoul, Republic of Korea. [5]Department of Neurology, Harvard Medical School and Brigham and Women's Hospital, The Center for Neurologic Diseases, Boston, Massachusetts, USA.

Macrophages characterized as M2 and M2-like regulate immune responses associated with immune suppression and healing; however, the relationship of this macrophage subset to CD169$^+$ tissue-resident macrophages and their contribution to shaping alloimmune responses is unknown. Here we identified a population of M2-like tissue-resident macrophages that express high levels of the phosphatidylserine receptor TIM-4 and CD169 (TIM-4^{hi}CD169$^+$). Labeling and tracking of TIM-4^{hi}CD169$^+$ macrophages in mice revealed that this population is a major subset of tissue-resident macrophages, homes to draining LNs following oxidative stress, exhibits an immunoregulatory and hypostimulatory phenotype that is maintained after migration to secondary lymphoid organs, favors preferential induction of antigen-stimulated Tregs, and is highly susceptible to apoptosis. Moreover, CD169$^+$ tissue-resident macrophages were resistant to oxidative stress–induced apoptosis in mice lacking TIM-4. Compared with heart allografts from WT mice, *Tim4*$^{-/-}$ heart allografts survived much longer and were more easily tolerized by non-immunosuppressed recipients. Furthermore, *Tim4*$^{-/-}$ allograft survival was associated with the infiltration of Tregs into the graft. Together, our data provide evidence that M2-like TIM-4^{hi}CD169$^+$ tissue-resident macrophages are immunoregulatory and promote engraftment of cardiac allografts, but their influence is diminished by TIM-4–dependent programmed cell death.

Introduction

Recent advances in macrophage biology have revealed several subpopulations. One prominent categorization separates Ly6C$^+$ monocyte-derived macrophages into M1 (destructive, inflammatory) and M2 (healing, immunoregulatory) subsets. Monocytes differentiate into an immunoregulatory M2 phenotype in response to IL-13 and IL-4 (1, 2) and are characterized by expression of the arginine-catabolizing enzyme arginase I and the mannose receptor CD206. M2 and M2-like macrophages are heterogeneous and exert a broad range of immunoregulatory and cytoprotective functions that promote wound healing, production of antiinflammatory effector molecules, and local suppression of innate and adaptive immunity (1, 2).

Macrophages have also been subdivided into an Ly6C$^-$ tissue-resident population, which patrols peripheral tissues, and an Ly6C$^+$ tissue-infiltrating population, which is recruited to inflammatory sites. In contrast to tissue-infiltrating macrophages that arise from Ly6C$^+$ monocytes, tissue-resident macrophages arise from Ly6C$^-$ precursors that seed peripheral tissues during early development and maintain their presence by homeostatic proliferation, as they are not replenished by circulating precursors (3). This homeostatic maintenance requires the transcription factor TRIB1 (4) and can rely on local production of IL-34 (5). A subset of tissue-resident macrophages expresses CD169 (6), a receptor for sialic acid also referred to as sialoadhesin and siglec-I. CD11b$^+$F4/80$^+$Ly6C$^-$ tissue-resident macrophages reside in unperturbed tissues and, similar to certain CD11b$^+$F4/80$^+$Ly6C$^+$ tissue-infiltrating macrophage subsets, can exert immunoregulatory or immunostimulatory functions (7–9).

In addition to their presence in peripheral tissues, CD169$^+$ macrophages are found in the marginal zone of secondary lymphoid organs, where they can promote immune tolerance to soluble antigens and antigens expressed by dead cells (10, 11). Paradoxically, CD169$^+$ tissue-resident macrophages, or subsets thereof, can also promote pathogenic central nervous system autoimmunity (12–14) and antitumor immunity (15). Although CD169$^+$ macrophages are present in many tissues, including skin (6), heart (16), and pancreas (17) in mice and lung, colon, and liver in humans (18), their role in shaping adaptive alloimmune responses and the potential for subpopulations remains enigmatic.

Here, we found that TIM-4 was highly expressed on a prominent subset of Ly6C$^-$CD169$^+$ tissue-resident macrophages with an immunoregulatory phenotype and function. As CD169$^+$ tissue-resident macrophages constitute a major component of tissue-resident APCs (6), we tested several hypotheses, including: (a) that a numerically prominent TIM-4^{hi}CD169$^+$ subset of Ly6C$^-$ tissue-resident macrophages migrates to secondary lymphoid organs upon stimulation, (b) that Ly6C$^-$TIM-4^{hi}CD169$^+$ macrophage survival is regulated by the expression of TIM-4, and (c) that the

Authorship note: Thomas B. Thornley and Zemin Fang contributed equally to this work.
Conflict of interest: The authors have declared that no conflict of interest exists.
Submitted: October 2, 2013; **Accepted:** May 22, 2014.
Reference information: *J Clin Invest*. 2014;124(8):3443–3454. doi:10.1172/JCI73527.

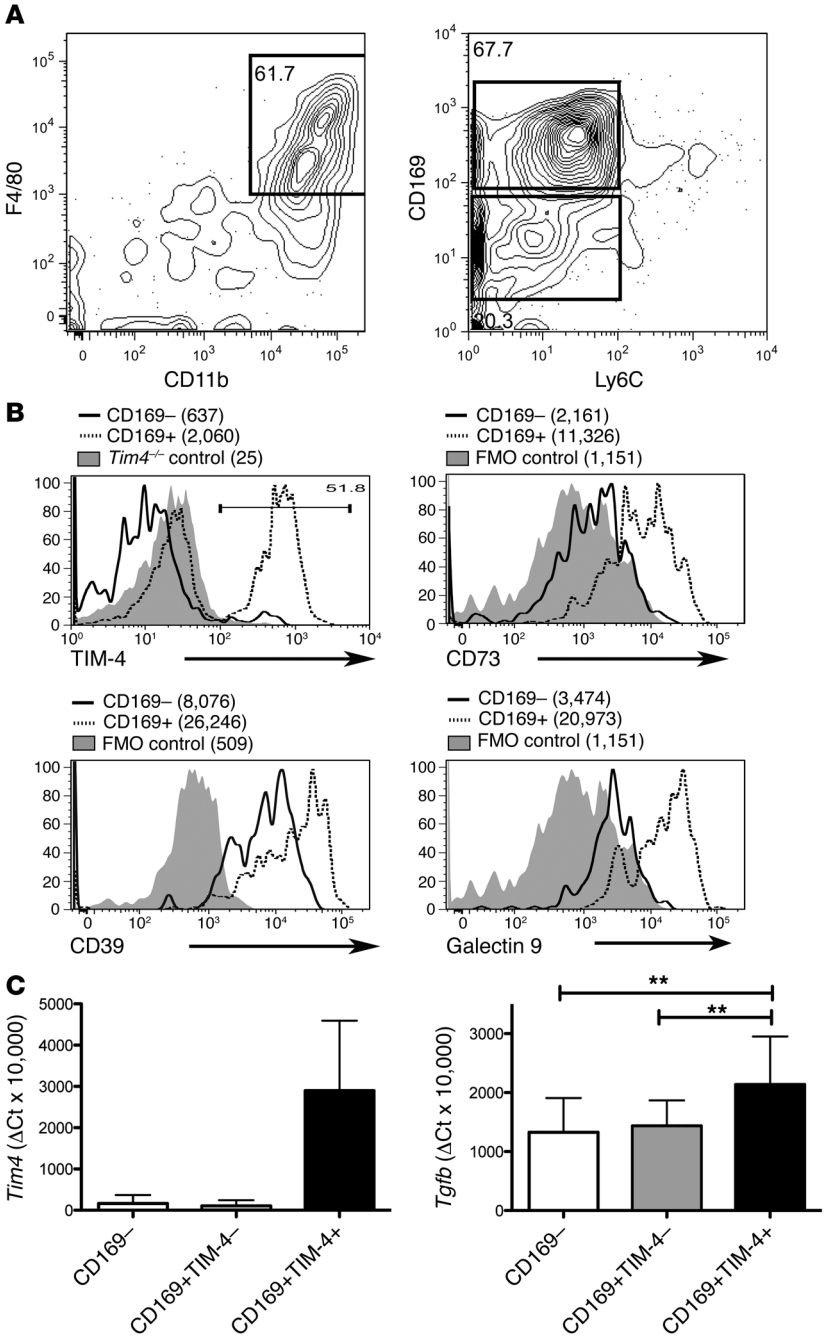

Figure 1. A subpopulation of skin-resident CD11b⁺F4/80⁺CD169⁺ tissue-resident macrophages with an immunoregulatory phenotype coexpresses TIM-4. Intradermal leukocytes were obtained from the skin of untreated C57BL/6 mice following collagenase digestion. Cells were stained with DAPI, anti-CD45, anti-F4/80, anti-CD11b, anti-CD169, and anti-Ly6C. (**A**) Using a sequential gating strategy, we gated on live (DAPI⁻) CD45⁺ cells (not shown) and then identified F4/80⁺CD11b⁺ cells that were then subdivided into Ly6C⁻ subpopulations that were CD169⁺ and CD169⁻. (**B**) DAPI⁻ CD11b⁺F4/80⁺Ly6C⁻CD169⁺ and DAPI⁻ CD11b⁺F4/80⁺Ly6C⁻CD169⁻ subsets of intradermal leukocytes were selected and assessed for the expression of TIM-4, CD39, CD73, and galectin-9 using the gating scheme shown in **A**. Shaded histograms represent fluorescence minus one (FMO) controls or anti–TIM-4–stained *Tim4*$^{-/-}$ skin macrophages. MFIs are noted parenthetically. (**C**) The CD169⁻, TIM-4$^{-/lo}$CD169⁺, and TIM-4^{hi}CD169⁺ subsets of the CD11b⁺F4/80⁺Ly6C⁻ population from **A** and **B** were cell sorted and analyzed by real-time PCR using the listed Taqman probes and primers. As expected, *Tim4* mRNA was expressed at high levels only in the TIM-4^{hi}CD169⁺ subpopulation ($P < 0.01$ among the 3 groups, 1-way repeated-measures ANOVA). *Tgfb* mRNA significantly differed between the TIM-4^{hi}CD169⁺ subpopulation and both TIM-4$^{-/lo}$ subsets. $^{**}P < 0.01$, 1-way repeated-measures ANOVA ($P < 0.01$) with Bonferroni post-test. Graphs represent mean ± SD from 7 unique animals from 3 independent experiments.

allograft donor TIM-4^{hi}CD169⁺ macrophage subset promotes immunoregulation, thereby prolonging cardiac allograft survival.

Results

The TIM-4^{hi}CD169⁺ phenotype defines a subset of tissue-resident macrophages that migrates to secondary lymphoid organs. CD45⁺CD11b⁺F4/80⁺Ly6C⁻ tissue-resident macrophages isolated from the skin of unmanipulated C57BL/6 mice included distinct CD169⁻ and CD169⁺ subsets (Figure 1A). Thus, we further analyzed the phenotype of CD11b⁺F4/80⁺Ly6C⁻CD169⁻ and CD11b⁺F4/80⁺Ly6C⁻CD169⁺ subpopulations. Interestingly, CD11b⁺F4/80⁺Ly6C⁻CD169⁺ tissue-resident macrophages expressed higher levels of galectin-9 (a molecule that binds to TIM-3 and triggers deletion of TIM-3⁺ Th1 cells; ref. 19) and of the ectoenzyme dephosphorylases CD39 and CD73 than did CD11b⁺F4/80⁺Ly6C⁻CD169⁻ cells (Figure 1B). Collectively, CD39 and CD73 cleave proinflammatory ATP and generate adenosine, a molecule with potent immunoinhibitory and immunoregulatory properties (20, 21). Notably, many CD45⁺CD11b⁺F4/80⁺Ly6C⁻CD169⁺ tissue-resident macrophages, but not all, expressed high levels of TIM-4 (~40%–50%; Figure 1B), a receptor for phosphatidylserine (22, 23) and TIM-1 (24). In contrast, all CD45⁺CD11b⁺F4/80⁺Ly6C⁻CD169⁻ skin-derived tissue-resident macrophages were TIM-4⁻ (Figure 1B).

Thus, skin CD11b⁺F4/80⁺ cells were quite heterogeneous, consisting of at least 3 tissue-resident Ly6C⁻ subpopulations: TIM-4⁻CD169⁻, TIM-4$^{-/lo}$CD169⁺, and TIM-4^{hi}CD169⁺. Strikingly, we

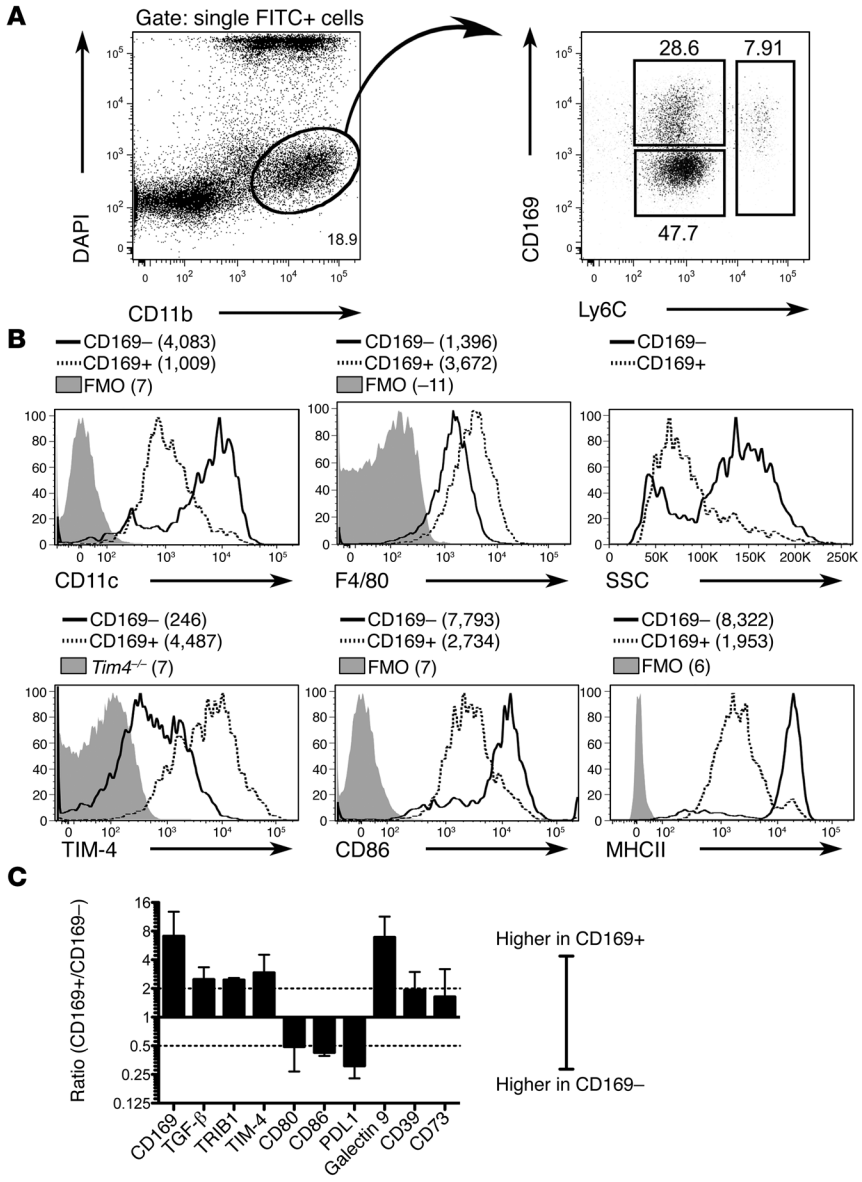

Figure 2. Oxidation-stressed TIM-4^{hi}CD169^{+} tissue-resident macrophages manifest a hypostimulatory phenotype relative to CD169^{-} APCs after migration to the dLN. (**A**) The abdominal and thoracic skin of shaven C57BL/6 WT mice was painted with 1% FITC in 1:1 dibutyl phthalate/acetone. 18 hours later, dLN cells were collected and stained with DAPI, anti-CD11b, anti-Ly6C, and anti-CD169. We identified tissue-emigrating (FITC^{+}) viable (DAPI^{-}) CD11b^{+} dLN cells, which harbored distinct Ly6C^{-}CD169^{+} and Ly6C^{-}CD169^{-} fractions that were subsequently analyzed for additional phenotypic characteristics. (**B**) We assessed DAPI^{-}FITC^{+}CD11b^{+}Ly6C^{-}CD169^{-} and DAPI^{-}FITC^{+}CD11b^{+}CD169^{+} dLN cells for expression of the indicated markers, which revealed a CD11c^{lo}F4/80^{hi}SSC^{lo} macrophage-like phenotype for Ly6C^{-}CD169^{+} dLN cells and a CD11c^{hi}F4/80^{lo}SSC^{hi} DC-like phenotype for Ly6C^{-}CD169^{-} dLN cells. Ly6C^{-}CD169^{+} macrophages expressed higher levels of TIM-4, but lower levels of CD86 and MHCII, compared with CD169^{-} APCs. Shaded histograms represent indicated controls. Plots are representative of 3 independent experiments. MFIs are indicated parenthetically. (**C**) CD169^{+} macrophages (FITC^{+}CD11b^{+}Ly6C^{-}CD169^{+}) and CD169^{-} APCs (FITC^{+}CD11b^{+}Ly6C^{-}CD169^{-}) were isolated from the dLN of FITC-painted mice by FACS sorting using the gates in **A** and analyzed by real-time PCR. The $\Delta Ct^{CD169+}/\Delta Ct^{CD169-}$ ratio (mean ± SD) is plotted for each transcript from 3 independent experiments on a $\log_2$ scale. Dashed lines are plotted at ± 2-fold differences.

found that the Ly6C^{-}TIM-4^{hi}CD169^{+} double-positive subpopulation from unperturbed skin expressed ~60% higher transcript levels of *Tgfb* than the Ly6C^{-}TIM-4^{-}CD169^{-} and Ly6C^{-}TIM-4$^{-/lo}$ CD169^{+} subpopulations (Figure 1C).

We hypothesized that TIM-4^{hi}CD169^{+} tissue-resident macrophages would migrate to secondary lymphoid organs following oxidative stress and exhibit an immunoregulatory phenotype at this critical site for T cell activation. To study tissue-resident rather than circulating macrophages, we used the FITC painting model, wherein fluorescently tagged intradermal APCs undergo oxidative stress following exposure to dibutyl phthalate (25, 26). Stimulation of intradermal APCs causes them to migrate to draining LNs (dLNs), where they are identified by the presence of FITC.

After 18 hours, we analyzed live (DAPI^{-}) tissue-derived (FITC^{+}) CD11b^{+} dLN cells by flow cytometry and found that, similar to cells derived from skin, this FITC^{+} dLN homing population bore distinct Ly6C^{-}CD169^{+} and Ly6C^{-}CD169^{-} fractions (Figure 2A). In contrast to Ly6C^{-}TIM-4^{int}CD169^{-} dLN cells, Ly6C^{-}CD169^{+} dLN cells were TIM-4^{hi} (Figure 2B). This also contrasted with the heterogeneity of CD11b^{+}Ly6C^{-}CD169^{+} tissue-resident macrophages extracted from tissue, which contained discrete TIM-4^{hi} and TIM-4$^{-/lo}$ subsets. Importantly, FITC^{+}CD11b^{+}Ly6C^{-}TIM-4^{hi}CD169^{+} macrophages in the dLN possessed an F4/80^{hi}CD169^{hi} phenotype that was not present in LNs of untreated mice (Supplemental Figure 1A; supplemental material available online with this article; doi:10.1172/JCI73527DS1). Moreover, FITC^{-}CD11b^{+}Ly6C^{-}TIM-4^{hi}CD169^{+} cells from FITC-painted mice were F4/80$^{lo/int}$CD169$^{lo/int}$, a phenotype similar to the resident CD11b^{+}Ly6C^{-}TIM-4^{hi}CD169^{+} dLN cells found in unpainted mice (Supplemental Figure 1A). These results strongly indicate that TIM-4^{hi}CD169^{+} tissue-resident macrophages migrated to the LN after inflammation-incited oxidative stress, rather than passively acquiring FITC. Only rare Ly6C^{+}CD169^{+} cells were found in the skin of untreated mice (Figure 1A) and were therefore not further characterized.

FITC^{+}CD11b^{+}Ly6C^{-}TIM-4^{int}CD169^{-} dLN cells (referred to hereafter as CD169^{-} APCs) were DC-like, expressing high CD11c but

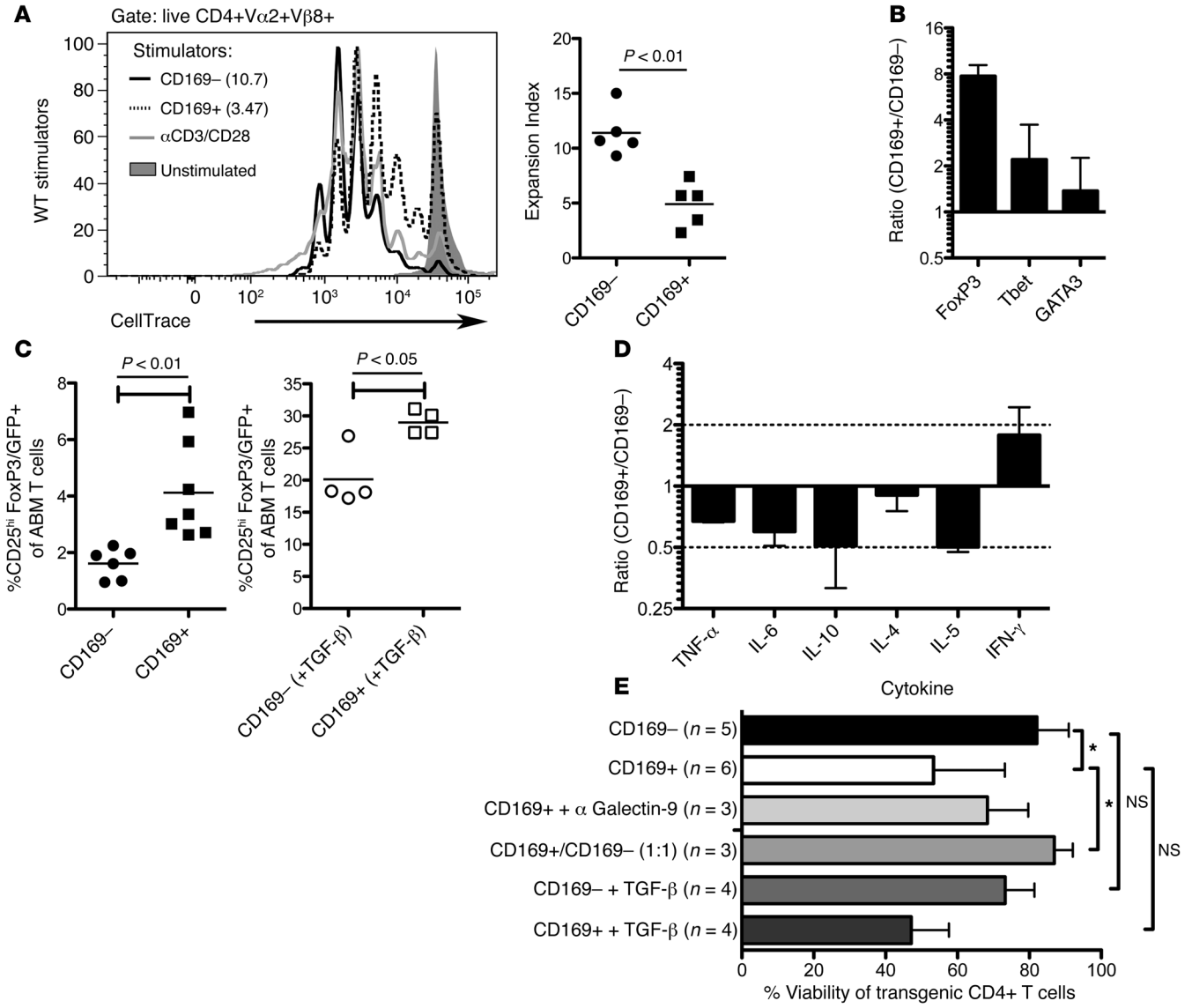

Figure 3. Compared with oxidation-stressed CD169⁻ APCs, oxidation-stressed TIM-4^{hi}CD169⁺ macrophages induce higher levels of FoxP3 transcripts, but inferior T cell survival. Live (DAPI⁻) CellTrace Violet–labeled ABM TCR transgenic T cells (DAPI⁻CD4⁺FoxP3/GFP⁻) were cocultured for 4 days with DAPI⁻FITC⁺CD11b⁺Ly6C⁻CD169⁻ APCs or DAPI⁻FITC⁺CD11b⁺Ly6C⁻CD169⁺ macrophages from the dLNs of WT FITC painted bm12 mice. (**A**) Proliferation in gated live CD4⁺ ABM TCR transgenic (Vα2⁺Vβ8⁺) T cells after 4 days of culture, shown in a histogram from a representative experiment. Expansion indices are indicated parenthetically as well as graphically. (**B**) The ratio of the indicated transcripts in CD169⁺ relative to CD169⁻ stimulated CD4⁺Vα2⁺Vβ8⁺ TCR transgenic T cells sorted on day 4, shown as mean ± SD from 2 independent experiments on a $\log_2$ scale. (**C**) Frequency (mean ± SD) of CD25^{hi}FoxP3/GFP⁺ cells within the gated CD4⁺Vα2⁺Vβ8⁺ population in MLRs treated without or with TGF-β (5 ng/ml), from 4–7 independent experiments. (**D**) Ratio of the indicated cytokines in CD169⁺ relative to CD169⁻ stimulated MLR cultures, shown as mean ± SD from 2 independent experiments on a $\log_2$ scale. Dashed lines are plotted at ±2-fold differences. (**E**) Percent viability (mean ± SD) of CD4⁺Vα2⁺Vβ8⁺ T cells from MLR cultures. *$P < 0.05$, 1-way ANOVA ($P < 0.05$) with Bonferroni post-test.

low F4/80 levels and exhibiting high side scatter (SSC). Conversely, FITC⁺CD11b⁺Ly6C⁻TIM-4^{hi}CD169⁺ dLN cells (referred to hereafter as TIM-4^{hi}CD169⁺ macrophages) expressed low levels of CD11c and high levels of F4/80 and CD11b, and exhibited low SSC (Figure 2B).

TIM-4^{hi}CD169⁺ macrophages that migrated to the dLN expressed siglec-H (Supplemental Figure 1B). However, the relationship of these cells to M2-like tissue-resident macrophages bearing siglec family members other than CD169, found in macrophages isolated from adipose (4) and lung (9) tissue, remains unclear.

TIM-4^{hi}CD169⁺ macrophages possess an antiinflammatory, immunoregulatory phenotype. As both the CD169⁺ and CD169⁻ subsets of skin-derived CD11b⁺F4/80⁺Ly6C⁻ cells migrated to the dLN, we interrogated the phenotype of these 2 dLN-homing populations. Compared with dLN-homing CD169⁻ APCs, TIM-4^{hi}CD169⁺ macrophages expressed lower levels of CD86 and MHCII proteins (Figure 2B). Transcriptional analysis confirmed lower expression of CD80, CD86, and MHCII antigen presentation molecules in TIM-4^{hi}CD169⁺ macrophages compared with CD169⁻ APCs in the dLN, but revealed an increase in the expression of galectin-9, TGF-β, and the ectoenzyme dephosphorylases CD39 and CD73 (Figure 2C). Increased expression of galectin-9 and CD73 cell surface protein were confirmed by flow cytometry

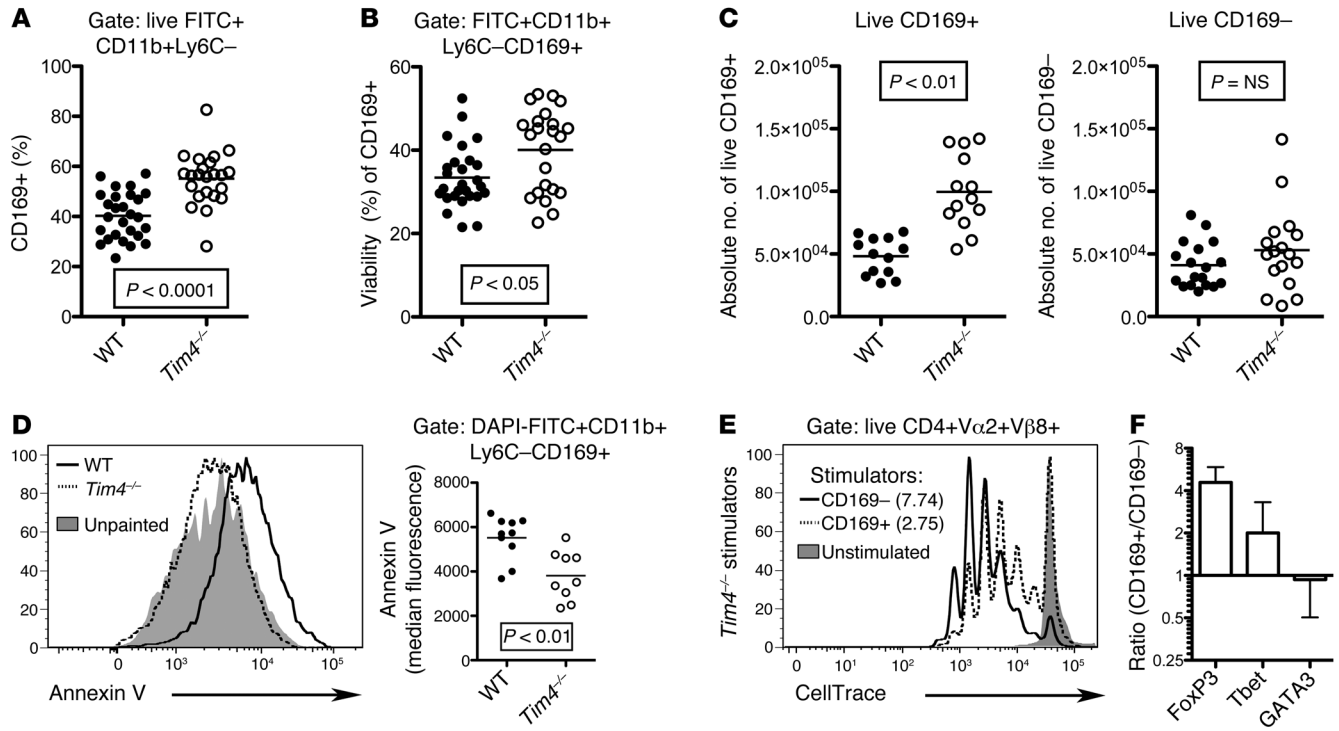

Figure 4. The presence of tissue-resident FITC$^+$CD11b$^+$Ly6C$^-$CD169$^+$ macrophages is increased in dLNs of *Tim4*$^{-/-}$ compared with WT mice after oxidative stress. (**A**) Higher frequency of DAPI$^-$FITC$^+$CD11b$^+$Ly6C$^-$ cells expressing CD169 in *Tim4*$^{-/-}$ versus WT dLNs 18 hours after FITC painting ($P < 0.0001$). (**B**) Higher percent viability of gated FITC$^+$CD11b$^+$Ly6C$^-$CD169$^+$ macrophages in *Tim4*$^{-/-}$ versus WT dLNs ($P < 0.05$), as determined by gate-exclusion of dead and dying cells (see Supplemental Figure 3A). (**C**) Higher absolute number of DAPI$^-$FITC$^+$CD11b$^+$Ly6C$^-$CD169$^+$ ($P < 0.01$), but not CD169$^-$ (P = NS), dLN cells in *Tim4*$^{-/-}$ versus WT FITC-painted mice. (**D**) *Tim4*$^{-/-}$ DAPI$^-$FITC$^+$CD11b$^+$Ly6C$^-$CD169$^+$ macrophages bound less annexin V than WT DAPI$^-$FITC$^+$CD11b$^+$Ly6C$^-$CD169$^+$ macrophages ($P < 0.01$). (**E**) CD4$^+$FoxP3/GFP$^-$ T cells from ABM TCR transgenic mice were sorted, labeled, and cocultured with CD169$^-$ APCs or CD169$^+$ macrophages from dLNs of FITC-painted *Tim4*$^{-/-}$ bm12 mice (as described in Figure 3A for WT bm12). Proliferation was reduced in ABM TCR transgenic T cells cultured with *Tim4*$^{-/-}$ CD169$^+$ versus CD169$^-$ MLR stimulator cells. Plots are representative of 3 independent experiments. Expansion indices are indicated parenthetically. (**F**) Ratio of the indicated transcripts in *Tim4*$^{-/-}$ CD169$^+$ versus CD169$^-$ stimulated CD4$^+$Vα2$^+$Vβ8$^+$ TCR transgenic T cells sorted on day 4 (mean ± SD from 2 independent experiments on a $\log_2$ scale).

(Supplemental Figure 1B). TIM-4^{hi}CD169$^+$ macrophages also expressed higher levels of the tissue-resident macrophage selective transcription factor TRIB1 (4) than did CD169$^-$ APCs (Figure 2C). Thus, cell surface expression of TIM-4, galectin-9, CD73, F4/80, and CD169, in addition to transcript expression of the transcription factor TRIB1 (4), identified a subset of tissue-resident macrophage that migrates to the dLN in response to oxidative stress. TIM-4^{hi}CD169$^+$ macrophages maintained a hypostimulatory and antiinflammatory phenotype compared with CD169$^-$ APCs after migration to secondary lymphoid organs. We speculate that it is the cumulative expression of multiple immunoregulatory molecules, and the hypoexpression of MHC and costimulatory proteins, rather than one individual immunoregulatory molecule, that gives these cells immunoregulatory potency. The precise contribution of each individual immunoregulatory molecule is difficult to assess in a system that is likely to be overdetermined.

TIM-4^{hi}CD169$^+$ macrophages promote greater Treg differentiation and proliferation in the mixed lymphocyte reaction than do CD169$^-$ APCs. Based on their hypostimulatory and antiinflammatory phenotype, we hypothesized that, compared with viable CD169$^-$ APCs, viable TIM-4^{hi}CD169$^+$ macrophages from the dLN would favor generation of Treg over effector T cell (Teff) responses when used as mixed lymphocyte reaction (MLR) stimulators. To test this hypothesis, we used the ABM TCR transgenic model system of alloreactivity (27). ABM TCR transgenic mice express a CD4$^+$ TCR transgene that recognizes the mutant MHC class II (MHCII) molecule I-A^{bm12} expressed by bm12 mice. Using ABM T cells that express GFP driven by the Treg promoter FoxP3 (FoxP3/GFP), we isolated CD4$^+$FoxP3/GFP$^-$ responder T cells and labeled them with CellTrace Violet. We then cultured these T cells for 4 days with DAPI$^-$ TIM-4^{hi}CD169$^+$ macrophages or with DAPI$^-$ CD169$^-$ APCs (which are TIM-4^{int}) isolated from the dLN of FITC-painted bm12 mice. Similar to C57BL/6 strains, DAPI$^-$FITC$^+$CD11b$^+$Ly6C$^-$CD169$^+$ cells from the dLN of FITC-painted bm12 mice expressed more TIM-4, CD73, and galectin-9, but less CD86, than did DAPI$^-$FITC$^+$CD11b$^+$Ly6C$^-$CD169$^-$ dLN cells (Supplemental Figure 2A). Interestingly, TIM-4^{hi}CD169$^+$ macrophages induced less T cell proliferation than did CD169$^-$ APCs (Figure 3A). A similar observation was noted when proliferation was assessed exclusively in transgenic T cells that express an early activation antigen (data not shown), which indicates that proliferation was also lower among transgenic T cells that had encountered antigen.

Strikingly, transcriptional analysis of transgenic MLR responder T cells from the aforementioned MLRs revealed that, compared with CD169$^-$ APCs, TIM-4^{hi}CD169$^+$ macrophages derived from the dLN of FITC painted mice induced amplified gene expression of the

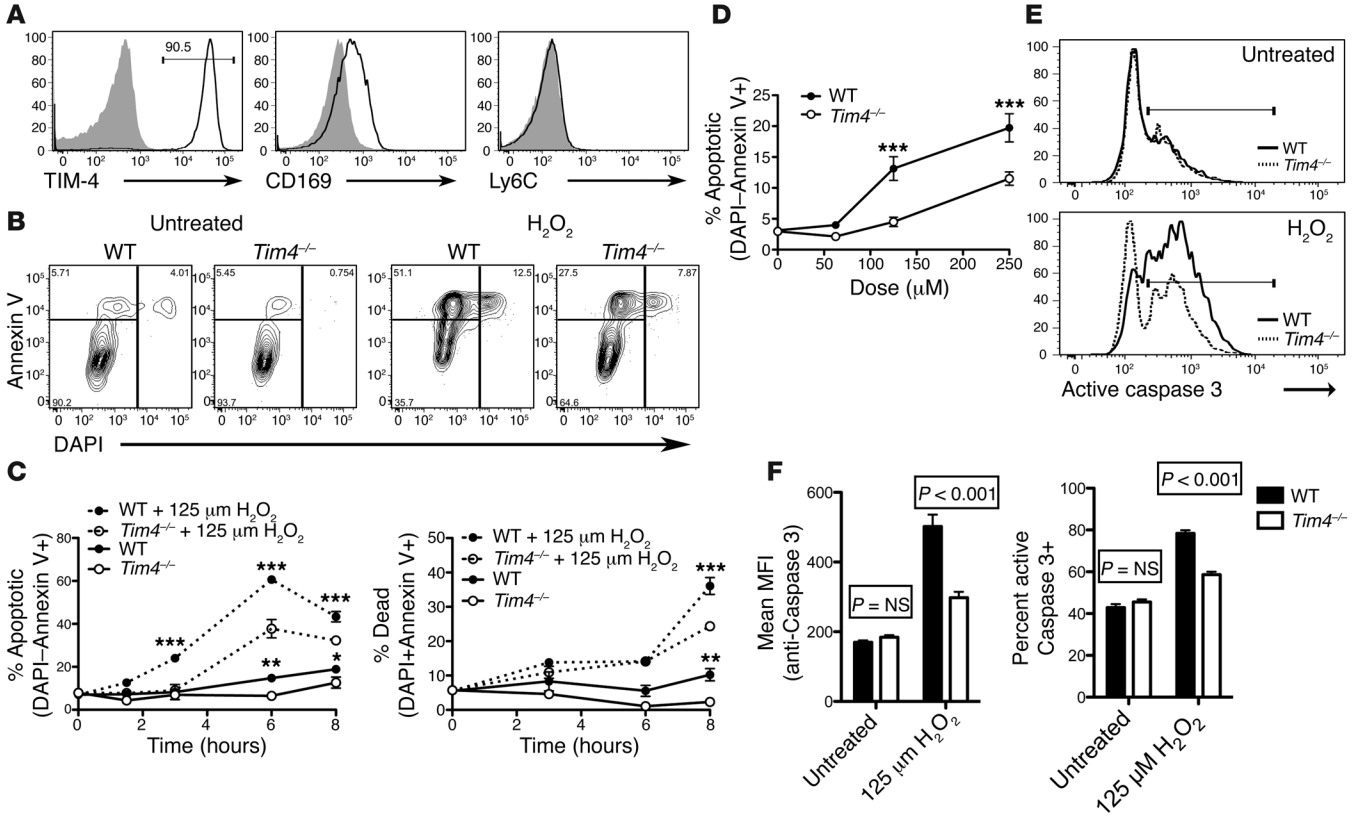

Figure 5. CD169⁺ peritoneal macrophages are resistant to H_2O_2-induced apoptosis in *Tim4*$^{-/-}$ relative to WT mice. (**A**) Histograms of gated WT or *Tim4*$^{-/-}$ DAPI$^-$CD11b$^+$F4/80$^+$ peritoneal macrophages revealed TIM-4 and CD169 expression, but not Ly6C expression. Shaded histograms represent indicated controls. MFI is noted parenthetically. (**B**–**D**) Gated WT or *Tim4*$^{-/-}$ CD11b$^+$F4/80$^+$ peritoneal macrophages incubated in the presence or absence of H_2O_2 (125 μM unless otherwise indicated) were analyzed for DAPI and annexin V binding by flow cytometry. (**B**) Representative flow cytometry plots at 3 hours after treatment. (**C**) Summary graphs from 1 of 3 independent experiments, showing lower apoptosis (DAPI$^-$annexin V$^+$) and cell death (DAPI$^+$annexin V$^+$) in *Tim4*$^{-/-}$ versus WT CD11b$^+$F4/80$^+$ macrophages. *P < 0.05, **P < 0.01, ***P < 0.001, ANOVA (P < 0.0001) with Bonferroni post-test. (**D**) Dose-response curve showing less apoptosis (DAPI$^-$annexin V$^+$) in *Tim4*$^{-/-}$ versus WT CD11b$^+$F4/80$^+$ macrophages at 3 hours. ***P < 0.001, ANOVA (P < 0.01) with Bonferroni post-test. (**E** and **F**) Gated CD11b$^+$F4/80$^+$ macrophages treated with 125 μM H_2O_2 for 3 hours were permeabilized and stained for intracellular active caspase-3 in triplicate. Shown are representative histograms (**E**) and summary graphs showing active caspase-3 MFI and frequency of active caspase-3$^+$ macrophages from 1 of 2 independent experiments (**F**). Active caspase-3 levels in gated *Tim4*$^{-/-}$ macrophages was reduced compared with WT macrophages. P values were determined by ANOVA (P < 0.01) with Bonferroni post-test. All graphs depict mean ± SEM from a representative experiment performed in triplicate.

immunoregulatory transcription factor FoxP3 relative to the Teff transcription factors Tbet and GATA3 in MLR responder T cells (Figure 3B). We also found an average 2.5-fold increase in FoxP3/GFP expression in T cells stimulated with CD169$^+$ versus CD169$^-$ MLR stimulator cells, as determined by GFP reporter expression (Figure 3C and Supplemental Figure 2B). This finding was consistent with the prior observation that lung-derived macrophages from uninflamed lungs promote FoxP3 expression (9). When used in a T-suppressor assay, unlabeled TCR transgenic CD4$^+$FoxP3/GFP$^+$ Tregs isolated from CD169$^+$ macrophage–stimulated MLR cultures suppressed the proliferation of TCR transgenic CD4$^+$FoxP3/GFP$^-$ responder T cells in response to T cell–depleted (CD90$^-$) bm12 splenocytes (Supplemental Figure 2C), demonstrating the regulatory activity of these cells. Thus, tissue-resident macrophages maintain immunoregulatory potential after stimulation and migration to the dLN.

TIM-4^{hi}CD169$^+$ macrophages engender poor overall T cell survival in the MLR relative to CD169$^-$ APCs. Consistent with our MLR proliferation data, we observed lower levels of TNF-α, IL-6, IL-10, IL-4, and IL-5 in the undiluted supernatants of TIM-4^{hi}CD169$^+$ macrophage–stimulated versus CD169$^-$ APC–stimulated MLR cultures (Figure 3D). There was, however, an increase in IFN-γ in TIM-4^{hi}CD169$^+$ macrophage–stimulated versus CD169$^-$ APC-stimulated MLR cultures (Figure 3D).

As IFN-γ (28–30) and galectin-9 (19) promote Th1 cell apoptosis and transplant tolerance, we measured the viability of TCR transgenic T cells in these MLR cultures. TIM-4^{hi}CD169$^+$ stimulator macrophages engendered poor T cell survival relative to CD169$^-$ stimulator APCs (Figure 3E). We cannot exclude the possibility that such alterations in viability may contribute to the observed reduction in effector cytokine production, or that decreased proliferation may affect the percent viability. Blockade with anti–galectin-9 caused a modest but statistically insignificant survival increase in TIM-4^{hi}CD169$^+$ macrophage-stimulated T cells, despite high relative expression of galectin-9 in this population. Thus, the contribution of galectin-9 to the observed T cell death is likely but one component of an overdetermined system in which multiple effector molecules have overlapping functions, thereby making it difficult to ascertain the absolute contribution of a specific molecule (30).

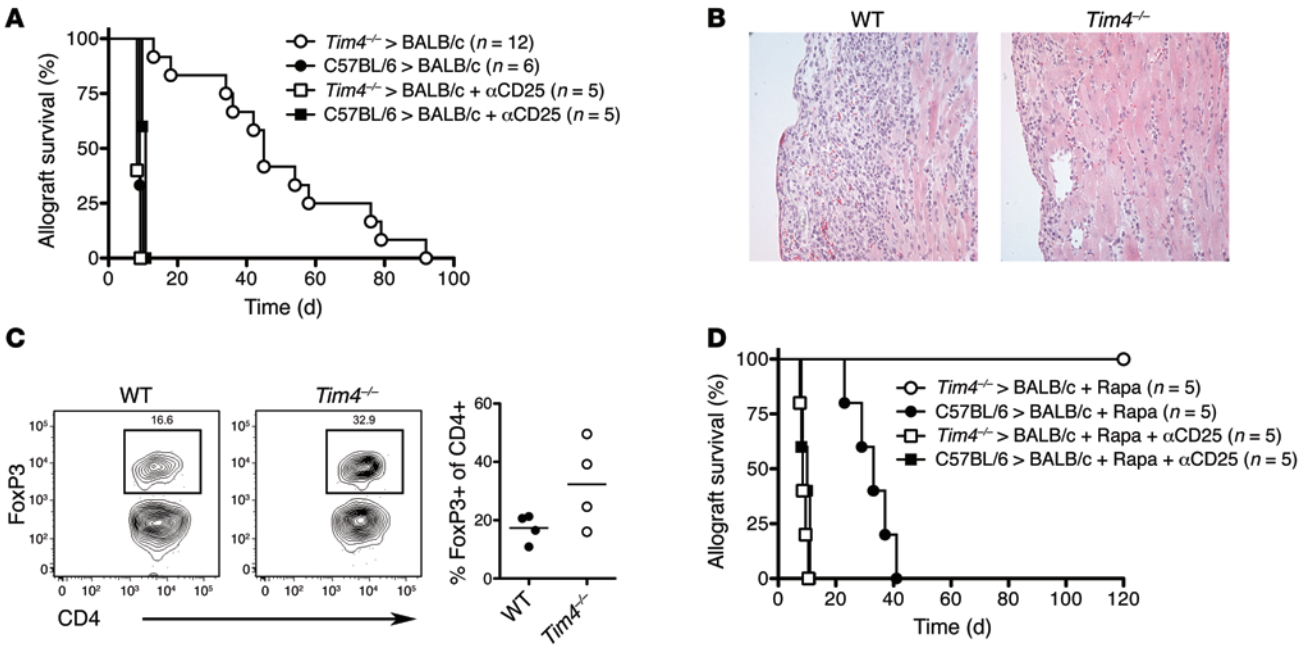

Figure 6. *Tim4*$^{-/-}$ heart allografts exhibit prolonged Treg-dependent transplant survival compared with WT allografts. (**A**) C57BL/6 WT and C57BL/6 *Tim4*$^{-/-}$ hearts were transplanted into fully allogeneic WT BALB/c mice, with or without Treg-depleting anti-CD25 treatment of recipients on day –1 relative to transplantation. The prolonged survival of allogeneic *Tim4*$^{-/-}$ versus WT heart allografts ($P < 0.0001$, log-rank Mantel-Cox analysis) was abrogated by anti-CD25 pretreatment of the recipients. (**B**) 7 days after transplantation, transplanted hearts were removed, formalin fixed, paraffin embedded, and stained with H&E. Original magnification, ×400. Images are representative of 5 fields observed from 3 independent transplanted hearts per group. (**C**) Graft-infiltrating mononuclear cells were isolated from WT or *Tim4*$^{-/-}$ heart allografts transplanted into BALB/c mice 7 days after transplantation. FoxP3 expression was detected in live (Live/Dead Blue^{-}) CD4^{+} T cells by intracellular staining. Shown are representative flow cytometry plots and summary graph. (**D**) Mice were transplanted as in **A**. Rapamycin treatment induced indefinite survival of *Tim4*$^{-/-}$ hearts, but merely prolonged survival of WT hearts ($P < 0.01$, log-rank Mantel-Cox analysis).

Next, we cultured ABM TCR transgenic T cells with a 1:1 mixture of CD169^{-} APCs and TIM-4^{hi}CD169^{+} macrophages. As viability was similar between the 1:1 mixture and pure CD169^{-} cultures (Figure 3E), the decrease in viability linked to TIM-4^{hi}CD169^{+} macrophages therefore arose from a mechanism that was counteracted or diluted by the presence of CD169^{-} APCs. Together, these data demonstrated that, compared with CD169^{-} APCs, the control of Teff responses by TIM-4^{hi}CD169^{+} macrophages is multifaceted and includes (a) greater induction of Tregs relative to other T cell subsets, (b) reduction of overall T cell proliferation, and (c) a higher rate of death among activated T cells.

Addition of TGF-β to these MLR cultures increased the frequency of CD4^{+} T cells expressing FoxP3 in cultures stimulated with TIM-4^{hi}CD169^{+} macrophages compared with CD169^{-} APCs (Figure 3C and Supplemental Figure 2B). Thus, even the addition of high levels of exogenous TGF-β did not put CD169^{-} APCs on par with TIM-4^{hi}CD169^{+} macrophages in their ability to induce Tregs. Hence, the immunoregulatory activity of these cells likely extends beyond TGF-β expression. T cells cultured in the presence of TGF-β and either TIM-4^{hi}CD169^{+} macrophages or CD169^{-} APCs exhibited viability similar to that of T cells cultured with the same APC population in the absence of TGF-β (Figure 3E).

TIM-4^{hi}CD169^{+} macrophages are highly susceptible to TIM-4–dependent apoptosis. Next, we FITC-painted the skin of WT and *Tim4*$^{-/-}$ mice and analyzed CD169 expression on DAPI^{-} FITC^{+}CD11b^{+}Ly6C^{-} cells that migrated to the dLN. Strikingly, *Tim4*$^{-/-}$ mice possessed a greater frequency of viable CD169^{+} macrophages in dLNs compared with WT mice (Figure 4A). Thus, while CD169^{+} macrophages expressed high levels of TIM-4 in WT mice, there was an increase in CD169^{+} cellularity in *Tim4*$^{-/-}$ mice, despite the absence of TIM-4 expression.

We hypothesized that the increase in CD169^{+} macrophage frequency observed in the dLN of FITC-painted *Tim4*$^{-/-}$ mice was due to a decrease in TIM-4–dependent apoptotic death of CD169^{+} macrophages. In support of this hypothesis, CD169^{+} macrophage viability was found to be significantly higher in *Tim4*$^{-/-}$ mice than WT mice, as determined by analyses that excluded cells undergoing shrinkage (low forward scatter) or failed to exclude viability dyes (Figure 4B and Supplemental Figure 3A). We also observed an increase in the absolute number of viable CD169^{+} macrophages in dLNs of *Tim4*$^{-/-}$ mice (Figure 4C). In contrast, there was no significant difference in the absolute number of viable CD169^{-} APCs obtained from the dLNs of WT and *Tim4*$^{-/-}$ FITC-painted hosts (Figure 4C), despite low to intermediate expression of TIM-4 by these cells.

WT CD169^{+} macrophages from the dLN of FITC-painted mice bound annexin V, a marker for cells undergoing programmed cell death, more intensely than did *Tim4*$^{-/-}$ CD169^{+} macrophages (Figure 4D), which suggests that, among cells that migrate to the dLN, WT TIM-4^{hi}CD169^{+} tissue-resident macrophages are more susceptible to apoptosis than are *Tim4*$^{-/-}$ CD169^{+} tissue-resident macrophages. In contrast, the proportion of CD169^{+} cells expressing the Ki-67 proliferation-specific antigen was similar in WT and *Tim4*$^{-/-}$ CD169^{+} macrophages (Supplemental Figure 3B). Thus, the

greater number of CD169$^+$ macrophages in *Tim4*$^{-/-}$ versus WT mice was attributable to an increase in survival rather than proliferation.

It seems paradoxical that immunoregulatory CD169$^+$ macrophages express high levels of TIM-4, a potent costimulator of TIM-1$^+$ T cells (24, 31, 32). We therefore hypothesized that TIM-4 expression decreases the survival, but does not compromise the immunoregulatory potential, of this population. To test this hypothesis, we isolated CD169$^+$ macrophages and CD169$^-$ APCs from the dLNs of FITC-painted *Tim4*$^{-/-}$ bm12 mice and cultured them in the MLR with ABM TCR transgenic T cells, a short-term system in which APC survival is unlikely to play a significant role. Like WT TIM-4^{hi}CD169$^+$ macrophage stimulator cells, *Tim4*$^{-/-}$ CD169$^+$ macrophage stimulator cells supported less T cell proliferation compared with *Tim4*$^{-/-}$ CD169$^-$ APCs (Figure 4E and Supplemental Figure 2D). Interestingly, 1-way ANOVA showed no significant difference in proliferation between WT and *Tim4*$^{-/-}$ CD169$^+$ macrophages or between WT and *Tim4*$^{-/-}$ CD169$^-$ APCs. Compared with *Tim4*$^{-/-}$ CD169$^-$ APCs, *Tim4*$^{-/-}$ CD169$^+$ macrophage stimulator cells also induced enhanced FoxP3 transcript expression, as well as FoxP3/GFP transgene reporter expression, by responder T cells, compared with Tbet and GATA3 transcript expression (Figure 4F and Supplemental Figure 2, B and E). Thus, the expression of TIM-4 on CD169$^+$ macrophages negatively influenced their survival, but did not grossly dilute their immunoregulatory potential.

Tim4$^{-/-}$ *CD169*$^+$ *peritoneal macrophages are resistant to* H_2O_2*-induced cell death relative to WT CD169*$^+$ *peritoneal macrophages*. We sought to compare apoptotic susceptibility of WT and *Tim4*$^{-/-}$ tissue-resident macrophages in a controlled in vitro assay system. As isolation of TIM-4$^+$ tissue-resident macrophages from skin yields very few viable cells, the procedure for digesting tissues using collagenase proving particularly detrimental to tissue-resident cell viability (data not shown), we chose to assay peritoneal macrophages that express TIM-4. Like Ly6C$^-$CD169$^+$ skin-dwelling macrophages, all F4/80$^+$CD11b$^+$ peritoneal macrophages were Ly6C$^-$ and CD169$^+$, as well as CD39$^+$ and CD73$^+$, and most expressed TIM-4 (~85%–90%; Figure 5A and Supplemental Figure 4A), which demonstrated that peritoneal resident macrophages share at least 7 phenotypic markers in common with skin tissue-resident macrophages. To determine whether TIM-4 ablation reduces peritoneal macrophage apoptosis induced by oxidative stress ex vivo, we treated WT and *Tim4*$^{-/-}$ peritoneal exudate cells with the oxidative stressor H_2O_2. H_2O_2 is one of several reactive oxygen species that is generated as a part of most oxidation stress responses, including the responses to phthalates used in FITC painting (33) and ischemia-reperfusion injury (IRI) associated with transplantation (34). Strikingly, treatment with 125 μM H_2O_2 rendered *Tim4*$^{-/-}$ CD169$^+$ peritoneal macrophages resistant to H_2O_2-induced programmed cell death compared with WT peritoneal macrophages (Figure 5B). This resistance was conferred in a time- and dose-dependent manner (Figure 5, C and D, and Supplemental Figure 4B). Additionally, a decrease in caspase-3 activation in *Tim4*$^{-/-}$ versus WT macrophages was also noted in the presence of H_2O_2, but not in its absence (Figure 5, E and F). We therefore concluded that TIM-4 expression renders CD169$^+$ macrophages highly susceptible to apoptosis induced by oxidative stress, although it remains unclear whether TIM-4 plays a direct or indirect role in this process, as it does not possess an identified signaling domain (35). Nonetheless, the phenomenon is TIM-4 dependent.

Transplantation of Tim4$^{-/-}$ *heart allografts manifests prolonged Treg-dependent survival compared with WT heart allografts*. Using *Tim4*$^{-/-}$ mice as a tool, we tested the hypothesis that improved survival of CD169$^+$ tissue-resident macrophages migrating out of donor heart allografts, perhaps in response to IRI, would promote immunoregulation and allograft survival in the cardiac allograft transplantation model. In this model, we can selectively test the influence of donor tissue-resident macrophage cell survival on adaptive immunity, since it is possible to ablate TIM-4 in donor alloantigen-presenting tissue-resident macrophages without the confounding influences of TIM-4 deletion upon recipient circulating leukocytes. To this end, we transplanted WT or *Tim4*$^{-/-}$ C57BL/6 hearts into WT allogeneic BALB/c recipients. Similar to tissue-resident macrophages in skin, the vast majority of CD169$^+$ macrophages in WT transplanted hearts expressed high levels of TIM-4 (Supplemental Figure 5). Given that CD169, but not TIM-4, was present on tissue-resident macrophages in *Tim4*$^{-/-}$ donor hearts 3 days after transplantation, and that TIM-4 was present on CD169$^+$ tissue-resident macrophages in naive untransplanted WT hearts (Supplemental Figure 5), we concluded that the intragraft TIM-4^{hi}CD169$^+$ macrophages observed 3 days after transplantation were donor-derived rather than graft-infiltrating and did not require TIM-4 to develop.

Strikingly, *Tim4*$^{-/-}$ heart allografts survived longer than those of WT controls (median survival, 45 vs. 9 days; $P < 0.0001$; Figure 6A). Moreover, *Tim4*$^{-/-}$ bm12 skin allograft survival was prolonged compared with WT bm12 skin in ABM TCR transgenic recipients (Supplemental Figure 6A). While prolongation was not as dramatic in skin compared with heart transplants, this was expected, because skin allografts are widely known to be less amenable to tolerance induction or prolonged engraftment than other conventionally transplanted tissues (36). Assessment of the absolute number and viability of donor CD169$^+$ tissue-resident macrophages in transplanted tissues proved technically challenging, since few viable CD169$^+$ tissue-resident macrophages, in contrast to infiltrating recipient macrophages, could be recovered after collagenase digestion (data not shown).

The prolonged survival of *Tim4*$^{-/-}$ heart allografts was completely dependent on the presence of CD25$^+$ Tregs (Figure 6A). In parallel with prolonged allograft survival, fewer mononuclear and total CD3$^+$ T lymphocytes, but more Tregs, infiltrated *Tim4*$^{-/-}$ versus WT transplants 7 days after transplantation (Figure 6, B and C, and data not shown). Moreover, survival of *Tim4*$^{-/-}$, but not WT, heart allografts was prolonged indefinitely (>120 days) by the addition of a short, 2-week course of rapamycin treatment in transplant recipients (Figure 6D). Rapamycin treatment is known to enhance the differentiation of CD4$^+$ T cells to Tregs and facilitate the induction of transplant tolerance (37). In contrast to *Tim4*$^{-/-}$ donor hearts transplanted into WT recipients, WT hearts were rapidly rejected in both WT and *Tim4*$^{-/-}$ recipients (Supplemental Figure 6B).

Discussion

Recently, tissue-derived M2-like macrophages were noted to play important roles in regulating local innate (4) and adaptive (9) immune responses; however, the relationship between these M2-

like tissue-resident macrophages, typically Ly6C$^-$ cells, and the Ly6C$^-$CD169$^+$ tissue-resident macrophage subsets was not analyzed. The data reported herein led us to conclude that a TIM-4^{hi} Ly6C$^-$CD169$^+$ tissue-resident macrophage population: (a) constitutes a major subset of Ly6C$^-$ tissue-resident macrophages, (b) homes to dLNs, a major site for T cell activation, upon oxidative stress, (c) exhibits an immunoregulatory and hypostimulatory phenotype that is maintained after migration to dLNs, (d) favors preferential induction of antigen-stimulated Tregs, (e) is highly susceptible to apoptosis, and (f) is rendered resistant to apoptosis via genetic ablation of TIM-4 expression. As a consequence, *Tim4*$^{-/-}$ heart allografts placed into untreated recipients survived much longer than WT hearts and survived indefinitely with the addition of a short, suboptimal rapamycin treatment regimen. Inflammation creates a milieu in which there is oxidative stress. Thus, TIM-4^{hi}CD169$^+$ tissue-resident macrophages are immunoregulatory and hypostimulatory, but their long-term influence is diminished by their susceptibility to programmed cell death in response to oxidative stress.

Our data provided strong evidence that oxidation-stressed TIM-4^{hi}CD169$^+$ tissue-resident macrophages home to secondary lymphoid organs in sizeable numbers, where they likely influence adaptive immunity. Relative to CD169$^-$ APCs, TIM-4^{hi}CD169$^+$ macrophages exhibited a phenotype that was immunoregulatory, both in unperturbed tissue and after migration to the dLN, where they seem certain to encounter antigen-specific T cells. In contrast to CD169$^-$ APCs, TIM-4^{hi}CD169$^+$ macrophages expressed low levels of antigen presentation (MHCII) and costimulatory (CD80 and CD86) molecules, but higher levels of antiinflammatory (CD39, CD73, galectin-9, and TGF-β) molecules. Other immune cells with broad immunoregulatory properties, including Tregs (20), hematopoietic stem cells (38), and mesenchymal stem cells (39), express CD39 and CD73. As these cells express multiple immunoregulatory molecules, the principal effector molecule responsible immunoregulation expressed by a given CD39$^+$CD73$^+$ cell can vary from test system to test system.

Notably, TIM-4^{hi}CD169$^+$ macrophages expressed higher levels of the tissue-resident macrophage-associated transcription factor TRIB1 (4) than did CD169$^-$ APCs. Thus, dual cell surface expression of CD169 and TIM-4 serves as a key identifier of this population of tissue-resident M2-like macrophages after migration to secondary lymphoid organs. Their expression of high levels of CD169 and F4/80 also distinguishes migratory tissue-resident macrophages from TIM-4^{hi}CD169$^+$ macrophages found in the dLN of untreated mice. As we are presently unable to identify a single unique marker for the tissue-resident macrophage lineage, fate-mapping studies using ROSA26 reporter mice (40) are not possible at this time.

Stimulation by TIM-4^{hi}CD169$^+$ macrophages versus CD169$^-$ APCs has a profound influence on CD4$^+$ T cell proliferation, survival, and differentiation. In the MLR, compared with CD169$^-$ APCs, TIM-4^{hi}CD169$^+$ macrophage stimulator cells induced abundant expression of the immunoregulatory T cell transcription factor FoxP3, relative to the Teff transcription factors Tbet and GATA3. The ~2.5-fold increase in FoxP3/GFP expression in CD169$^+$ versus CD169$^-$ APC-stimulated T cells in the MLR was similar to our in vivo observations, as well as several other models of transplant tolerance in vivo and in vitro (41, 42). Moreover, TIM-4^{hi} CD169$^+$ macrophage stimulator cells severely compromised overall Teff survival (in contrast to the robust Teff survival generated by CD169$^-$ APCs), which changed the balance of Tregs and Teffs in favor of Tregs.

Despite high levels of TIM-4 expression on CD169$^+$ macrophages in WT FITC-painted mice, the abundance of CD169$^+$ cells was increased in *Tim4*$^{-/-}$ mice, despite their lack of TIM-4 expression. Moreover, genetic ablation of TIM-4 expression in CD169$^+$ peritoneal macrophages, ~85%–90% of which expressed TIM-4 in WT mice, rendered them resistant to oxidative stress–induced apoptosis. As TIM-4 lacks an intrinsic signaling domain (35, 43), it is likely that the role of TIM-4 is to bring dying cells that expose phosphatidylserine on their cell surface into close proximity with additional signal-inducing receptors.

TIM-4 expression was not assessed in previous studies detailing the important role of CD169$^+$ marginal zone macrophages in mediating tolerance to soluble and dead cell antigens (10, 11). Our data indicate that TIM-4 is necessary, but not necessarily sufficient, for the induction of apoptosis, and thus leads to apoptosis only when additional stimulation conferred by oxidative stress is encountered. In this way, immunoregulatory macrophages can be selectively eliminated when a potent immune response arises under inflammatory conditions. As TIM-4 lacks a signaling domain (35), it seems probable that TIM-4 plays an indirect role in macrophage apoptosis.

The immunoregulatory molecular phenotype of TIM-4^{hi} CD169$^+$ macrophages led us to speculate that, like activated TIM-3$^+$ Tregs (44), the survival of TIM-4^{hi}CD169$^+$ macrophages and their immunoregulatory potential is compromised in inflammatory settings. Strikingly, TIM-4^{hi}CD169$^+$ macrophages that migrate to dLNs are highly susceptible to apoptosis induced by oxidative stress, a feature of obvious importance to the long-term regulatory potential of these M2-like macrophages. The fragility of TIM-4^{hi} CD169$^+$ macrophages fits the model proposed for other cellular protagonists of immunoregulation: the immune system must eventually disarm immunoregulatory cells such that protective antimicrobial Teff responses in the given microenvironment are not unduly restrained. This fragility, however, becomes an obstacle under intense inflammatory conditions in which immunoregulation is desired. For example, transplanted allografts inevitably undergo oxidative stress as a consequence of IRI (45).

In IRI, a process inextricably associated with organ or tissue transplantation, it might be desirable to bolster survival of regulatory TIM-4^{hi}CD169$^+$ tissue-resident M2 macrophages. We observed a significant prolongation of heart allograft survival as a consequence of genetic TIM-4 ablation in donor cardiac and skin allografts. Moreover, a short course of suboptimal rapamycin therapy generated long-term CD25$^+$ T cell–dependent survival of *Tim4*$^{-/-}$, but not WT, allografts. Rapamycin is known to support Treg responses while suppressing Teff responses (46). As TIM-4 expression on WT CD169$^+$ macrophages did not compromise the immunoregulatory nature of CD169$^+$ tissue-resident macrophages in in vitro MLR assays, it seems more likely that genetic TIM-4 ablation promotes allograft survival by enhancing CD169$^+$ macrophage survival, rather than by blocking costimulation (21, 32, 33) of TIM-1$^+$ T cells by TIM-4^{hi} immunoregulatory macrophages. While we could

not demonstrate that improved survival of CD169$^+$ tissue-resident macrophages as a result of genetic TIM-4 ablation was directly responsible for Treg generation and transplant survival, as depletional studies are not possible at this time, our in vitro MLR results indicated that this is the most likely data-supported explanation.

The importance of CD169$^+$ tissue-resident macrophages in promoting allograft survival is consistent with data showing that the adoptive transfer of other M2-like macrophage subsets, such as Kupffer cells (47) or classic M2 macrophages differentiated from Ly6C$^+$ monocytes (48), prolong allograft survival. Our data are also consistent with the finding that the adoptive transfer of siglec-H$^+$ lung-derived macrophages suppresses asthmatic lung inflammation (9).

It was previously proposed that therapeutic anti–TIM-4 treatment inhibits CD4$^+$ T cells that express a TIM-4 ligand and that anti–TIM-4 could reduce proinflammatory cytokine secretion in bone marrow–derived macrophages (BMDMs) (49); however, the authors did not assess Ly6C$^-$CD169$^+$ tissue-resident macrophages, which differ considerably from BMDMs developmentally and functionally. Additionally, as we submitted this paper, an anti–TIM-4 mAb that does not discriminate between donor and recipient TIM-4 was shown to promote prolonged Treg-dependent skin allograft survival (41) by skewing Teff generation and promoting Tregs in response to CD11c$^+$ Flt3L-induced DCs. However, the use of splenic CD11c$^+$ stimulators makes it unclear whether this is a result of a change in DC phenotype or an alteration in the constituent subsets within the CD11c$^+$ population. It is possible that TIM-4 blockade may act through multiple, distinct mechanisms on tissue-resident macrophages, BMDMs, and DCs. It is also possible that antibody blockade and genetic blockade of TIM-4 function through different mechanisms.

Ly6C$^+$ macrophages contain a CD169$^+$ subset (Figure 2A), as does a small subset of DCs that resides outside of the marginal zone in secondary lymphoid organs (50). The use of a transplantation model enabled us to assess the effect of tissue-derived, alloantigen-expressing (donor) versus blood-derived (recipient) macrophage populations. Our results clearly demonstrated that donor-derived alloantigen-expressing TIM-4^{hi}CD169$^+$ tissue-patrolling macrophages play an important immunoregulatory role in the alloimmune response in vivo.

We conclude that TIM-4^{hi}CD169$^+$ tissue-resident macrophages, but not TIM-4$^{-/lo}$CD169$^+$ tissue-resident APCs, migrate to the dLN and possess an immunoregulatory phenotype that is maintained upon migration to the dLN. This subset of tissue-resident macrophages promotes immunoregulatory adaptive immunity in vitro and in vivo; however, these cells are highly susceptible to TIM-4–dependent, stress-induced apoptosis. Genetic ablation of *Tim4* reduced the susceptibility of CD169$^+$ tissue-resident macrophages to stress-induced apoptosis. As a likely consequence of this ablation, we observed an increase in the prominence of intragraft Tregs and improved *Tim4*$^{-/-}$ heart transplant survival in vivo. Thus, the survival or demise of TIM-4^{hi}CD169$^+$ macrophages is an important feature in determining the outcome of the allograft response and, almost certainly, other tissue-based immune responses.

Methods

Further information can be found in Supplemental Methods.

Mice. WT male C57BL/6J and BALB/cJ mice were obtained from Jackson Laboratories. C57BL/6 *Tim4*$^{-/-}$ mice were described previously (51). WT bm12 [*B6(C)-H2-Ab1*^{bm12}*/HkEgJ*] mice were obtained from Jackson Laboratories and crossed with *Tim4*$^{-/-}$ mice to generate *Tim4*$^{-/-}$ bm12 mice as described below. ABM TCR transgenic mice bearing the FoxP3/GFP reporter were bred in our facility (27).

Phenotypic analysis of skin-derived tissue-resident macrophages. Shaven skin from untreated mice was cut into small 1- to 2-mm fragments, then digested for 20 minutes in RPMI with 10% FBS and 1 mg/ml collagenase D or 0.07 mg/ml Liberase DL (Roche Applied Science). Fragments were passed through a metal sieve with light agitation and sequentially passed through 70- and 40-μm nylon filters. No ficoll gradient purification was performed for skin samples. Cells were then stained and analyzed by flow cytometry.

FITC painting. FITC painting was performed by applying 0.5 ml of 1% FITC (Sigma-Aldrich) in 1:1 acetone/dibutyl phthalate (Sigma-Aldrich) to the abdomen and thorax of shaven mice as described previously (52). 18 hours after application, the dLNs were collected, prepared into single-cell suspensions, and analyzed by flow cytometry as described below.

Antibodies, flow cytometry, and cell sorting. Single-cell suspensions were prepared, incubated with anti-CD32/CD16 (Fc Block; BD Biosciences), and stained with the indicated viability dye and antibodies. The following monoclonal antibodies were used: anti-CD4 (GK1.5; BioLegend), anti–TCR Vβ8.1/8.2 (KJ6-133.18; BioLegend), anti–TCR Vα2 (B20.1; BioLegend), anti-CD11b (M1/70; BioLegend), anti-F4/80 (BM8; BioLegend), anti-CD11c (N418; BioLegend), anti-CD169 (3D6.112; BioLegend), anti–TIM-4 (5G3; BioLegend), anti-CD86 (GL-1; BioLegend), anti–I-Ab (AF6-120.1; BioLegend), anti–siglec-H (551; BioLegend), anti-CD73 (TY/11.8; BioLegend), anti–galectin-9 (RG9-35; BioLegend), anti–caspase-3 active form (C92-605; BD Biosciences), anti-FoxP3 (FJK-16s; eBioscience). Live/Dead Blue or Yellow Fixable Stains (Life Technologies), Fixable Viability Dye eFluor 780 (eBioscience), or DAPI (BioLegend) was used to assess viability. Intracellular staining for activate caspase-3 was performed after extracellular staining using BD Cytofix/Cytoperm reagents (BD Biosciences). Staining for intracellular FoxP3 was performed after extracellular staining and subsequent permeabilization with FoxP3 fixation/permeabilization reagents (eBioscience). Data acquisition was performed on a special-order 5-laser LSRII flow cytometer (BD Biosciences). Cells were sorted using a FACS Aria or Aria II (BD Biosciences). In all sorting experiments, as well as analysis of dLN APCs, we applied 3 successive singlet gates to avoid including doublets (SSC-A/SSC-H, SSC-H/SSC-W, and FSC-H/FSC-W). Purity after sorting was routinely >97%. Analyses, including the embedded Expansion Index algorithm, were performed using FlowJo software (Tree Star).

MLR. DAPI$^-$FITC$^+$CD11b$^+$Ly6C$^-$ CD169$^+$ macrophages and CD169$^-$ APCs were isolated from FITC-painted WT or *Tim4*$^{-/-}$ bm12 mice. 2.5×10^4 sorted APCs were incubated with 10^5 sorted ABM CD4$^+$FoxP3/GFP$^-$ T cells labeled with CellTrace Violet (Life Technologies) in round-bottomed 96-well plates. For 1:1 mixed APC experiments, 2.5×10^4 cells from each subset were combined. Media was IMDM (Thermo Fisher Scientific) supplemented with 10% heat-inactivated FBS (Atlanta Biologics), 20 ng/ml IL-2 (Biolegend), penicillin/streptomycin/L-glutamine (Lonza), and Mycozap Plus-PR (Lonza). Plate-bound anti-CD3–stimulated (10 μg/ml) and soluble anti-CD28–stimulated (5 μg/ml) cultures were performed in flat-bottomed

96-well plates. After 96 hours, live ABM $CD4^+V\alpha2^+V\beta8^+$ transgenic T cells were sorted and analyzed by real-time PCR (see below). Viability was measured using Live/Dead Blue or Yellow (Invitrogen) or eFluor 780 fixable viability stain (eBioscience). Anti–galectin-9–treated wells were supplemented with 50 μg/ml purified Low Endotoxin Azide Free (LEAF) anti–galectin-9 (RG9-35; BioLegend).

Measurement of cytokines. Cytokines were measured in the supernatants of MLR cultures using mouse Th1/Th2 and mouse inflammation Cytometric Bead Arrays (BD Biosciences). The concentrations of the experimental samples were determined by interpolating their value from a standard curve generated from the MFIs of the provided standards. The ratio of select cytokines present in supernatants of MLR cultures in which ABM T cells were stimulated by either allogeneic $CD169^+$ or $CD169^-$ APCs was calculated ($CD169^+/CD169^-$), then plotted on a $\log_2$ axis.

Real-time PCR. The indicated T cells or APCs were sorted directly into lysis buffer RLT (Qiagen). RNA was extracted from isolated cells using the RNeasy Micro Kit (Qiagen). cDNA was generated using the TaqMan High Capacity Reverse Transcription Kit (Applied Biosystems). cDNA was analyzed by real-time PCR using the SYBR green method (SA Biosciences or Life Technologies) on a StepOne real-time PCR thermocycler (Life Technologies). Data were normalized to the *Gapdh* housekeeping control gene and using the ΔCt method of quantitation. Transcript ratios ($\Delta Ct^{CD169+}/\Delta Ct^{CD169}$) were calculated and plotted on a $\log_2$ axis. Primer sequences are provided in Supplemental Table 1.

Measurement of peritoneal macrophage apoptosis by flow cytometry. Peritoneal exudate cells were collected by peritoneal lavage using 5 ml IMDM media (Thermo Fisher Scientific) supplemented with 10% FBS (Atlanta Biologics). For flow cytometric measurement, 0.1 ml containing 5×10^4 cells was seeded into 5-ml FACS tubes or 2-ml polypropylene cluster tubes and treated with the indicated concentration of H_2O_2 (Sigma-Aldrich) for the indicated times. Cells were then stained with anti-F4/80, anti-CD11b, DAPI, and annexin V (BioLegend) in culture medium containing Ca^{2+} and Mg^{2+}, without washing, and analyzed 15 minutes later by flow cytometry.

Heterotopic heart transplantation. Heterotopic heart transplantation was performed as described previously (42) using male BALB/cJ recipients and age-matched male C57BL/6J WT or male C57BL/6 *Tim4*$^{-/-}$ donors. Anti-CD25 (0.25 mg, clone PC-61.5.3; Bio X Cell) monoclonal antibody was administered on day –1 relative to transplantation. Rapamycin (3 mg/kg, Henry Schein) was administered daily on days 0–6 relative to transplantation, then every other day until day 13 (42). Transplant viability was assessed daily by abdominal palpation. Rejection was defined as the day on which contractility ceased completely. Cessation of cardiac function was verified by visually inspecting the allograft.

Isolation of mononuclear leukocytes from heart transplants. Mononuclear cells were isolated from transplanted cardiac grafts by collagenase digestion and ficoll gradient purification as described previously (53). Briefly, extracted hearts were cut into small 1- to 2-mm fragments, digested for 20 minutes in RPMI (Thermo Fisher Scientific) with 10% FBS (Atlanta Biologics) and 1 mg/ml collagenase D (Sigma-Aldrich), purified by ficoll (Sigma-Aldrich) gradient centrifugation, stained with anti-CD4 and Live/Dead Blue, permeabilized, stained with anti-FoxP3, and then analyzed by flow cytometry.

Statistics. Statistical analyses were performed with Prism software (GraphPad). 2 means were compared using nonparametric 2-tailed Mann-Whitney *t* test. 3 or more means were compared using 1- or 2-way ANOVA with Bonferroni post-test. Allograft survival curves were generated by the Kaplan-Meier method and compared using log-rank Mantel-Cox statistical analysis. Allograft survival duration is presented as median survival time. In all cases, a *P* value less than 0.05 was considered significant.

Study approval. All mice were certified to be specific pathogen–free and cared for in accordance with the guidelines of the Institutional Animal Care and Use Committee at Beth Israel Deaconess Medical Center (Boston, Massachusetts, USA).

Acknowledgments

We thank Vasilis Toxavidis, John Tigges, Heidi Mariani, Sarah Schuett, Marissa Fahlberg, and Kaitlin Groglio for their expertise and assistance with flow cytometry and cell sorting. This work was funded by the National Institute of Allergy and Infectious Disease (grant 5P01AI073748, to T.B. Strom and V.K. Kuchroo), the Juvenile Diabetes Research Foundation (grant 3-2010-792, to T.B. Thornley), the National Institute of Diabetes and Digestive and Kidney Diseases (grant 5R01DK096138, to T.B. Strom, M. Koulmanda, and V.K. Kuchroo), and the National Heart, Lung, and Blood Institute (training grant T32HL007893, to T.B. Thornley).

Address correspondence to: Terry B. Strom, Beth Israel Deaconess Medical Center, The Transplant Institute, 330 Brookline Ave E/CLS-Room 608, Boston, Massachusetts 02215, USA. Phone: 617.735.2880; E-mail: tstrom@bidmc.harvard.edu.

1. Lawrence T, Natoli G. Transcriptional regulation of macrophage polarization: enabling diversity with identity. *Nat Rev Immunol*. 2011;11(11):750–761.
2. Murray PJ, Wynn TA. Protective and pathogenic functions of macrophage subsets. *Nat Rev Immunol*. 2011;11(11):723–737.
3. Hashimoto D, et al. Tissue-resident macrophages self-maintain locally throughout adult life with minimal contribution from circulating monocytes. *Immunity*. 2013;38(4):792–804.
4. Satoh T, et al. Critical role of Trib1 in differentiation of tissue-resident M2-like macrophages. *Nature*. 2013;495(7442):524–528.
5. Wang Y, et al. IL-34 is a tissue-restricted ligand of CSF1R required for the development of Langerhans cells and microglia. *Nat Immunol*. 2012;13(8):753–760.
6. Dupasquier M, Stoitzner P, van Oudenaren A, Romani N, Leenen P. Macrophages and dendritic cells constitute a major subpopulation of cells in the mouse dermis. *J Invest Dermatol*. 2004;123(5):876–885.
7. O'Neill AS, van den Berg TK, Mullen GE. Sialoadhesin — a macrophage-restricted marker of immunoregulation and inflammation. *Immunology*. 2013;138(3):198–207.
8. Martinez-Pomares L, Gordon S. $CD169^+$ macrophages at the crossroads of antigen presentation. *Trends Immunol*. 2012;33(2):66–136.
9. Soroosh P, et al. Lung-resident tissue macrophages generate Foxp3+ regulatory T cells and promote airway tolerance. *J Exp Med*. 2013;210(4):775–788.
10. Miyake Y, Asano K, Kaise H, Uemura M, Nakayama M, Tanaka M. Critical role of macrophages in the marginal zone in the suppression of immune responses to apoptotic cell-associated antigens. *J Clin Invest*. 2007;117(8):2268–2278.
11. McGaha TL, Chen Y, Ravishankar B, van Rooijen N, Karlsson MC. Marginal zone macrophages suppress innate and adaptive immunity to apoptotic cells in the spleen. *Blood*. 2011;117(20):5403–5412.
12. Wu C, et al. Sialoadhesin-positive macrophages bind regulatory T cells, negatively controlling their expansion and autoimmune disease progression. *J Immunology*. 2009;182(10):6508–6524.
13. Ip CW, Kroner A, Crocker PR, Nave KA, Martini R.

Sialoadhesin deficiency ameliorates myelin degeneration and axonopathic changes in the CNS of PLP overexpressing mice. *Neurobiol Dis*. 2007;25(1):105–111.
14. Kobsar I, Oetke C, Kroner A, Wessig C, Crocker P, Martini R. Attenuated demyelination in the absence of the macrophage-restricted adhesion molecule sialoadhesin (Siglec-1) in mice heterozygously deficient in P0. *Mol Cell Neurosci*. 2006;31(4):685–691.
15. Asano K, et al. CD169-positive macrophages dominate antitumor immunity by crosspresenting dead cell-associated antigens. *Immunity*. 2011;34(1):85–180.
16. Harel-Adar T, Ben Mordechai T, Amsalem Y, Feinberg M, Leor J, Cohen S. Modulation of cardiac macrophages by phosphatidylserine-presenting liposomes improves infarct repair. *Proc Natl Acad Sci U S A*. 2011;108(5):1827–1859.
17. Jansen A, Homo-Delarche F, Hooijkaas H, Leenen P, Dardenne M, Drexhage H. Immunohistochemical characterization of monocytes-macrophages and dendritic cells involved in the initiation of the insulitis and beta-cell destruction in NOD mice. *Diabetes*. 1994;43(5):667–742.
18. Hartnell A, Steel J, Turley H, Jones M, Jackson D, Crocker P. Characterization of human sialoadhesin, a sialic acid binding receptor expressed by resident and inflammatory macrophage populations. *Blood*. 2001;97(1):288–296.
19. Zhu C, et al. The Tim-3 ligand galectin-9 negatively regulates T helper type 1 immunity. *Nat Immunol*. 2005;6(12):1245–1252.
20. Deaglio S, et al. Adenosine generation catalyzed by CD39 and CD73 expressed on regulatory T cells mediates immune suppression. *J Exp Med*. 2007;204(6):1257–1265.
21. Eltzschig HK, Sitkovsky MV, Robson SC. Purinergic signaling during inflammation. *N Engl J Med*. 2013;368(13):1260.
22. Kobayashi N, et al. TIM-1 and TIM-4 glycoproteins bind phosphatidylserine and mediate uptake of apoptotic cells. *Immunity*. 2007; 27(6):927–940.
23. Miyanishi M, Tada K, Koike M, Uchiyama Y, Kitamura T, Nagata S. Identification of Tim4 as a phosphatidylserine receptor. *Nature*. 2007; 450(7168):435–439.
24. Meyers JH, et al. TIM-4 is the ligand for TIM-1, and the TIM-1-TIM-4 interaction regulates T cell proliferation. *Nat Immunol*. 2005;6(5):455–464.
25. Lee E, et al. Effect of di(n-butyl) phthalate on testicular oxidative damage and antioxidant enzymes in hyperthyroid rats. *Environ Toxicol*. 2007;22(3):245–255.
26. Corton JC, Lapinskas PJ. Peroxisome proliferator-activated receptors: mediators of phthalate ester-induced effects in the male reproductive tract? *Toxicol Sci*. 2005;83(1):4–17.
27. D'Addio F, et al. The link between the PDL1 costimulatory pathway and Th17 in fetomaternal tolerance. *J Immunol*. 2011;187(9):4530–4541.
28. Liu Y, Janeway C. Interferon gamma plays a critical role in induced cell death of effector T cell: a possible third mechanism of self-tolerance. *J Exp Med*. 1990;172(6):1735–1739.
29. Markees TG, et al. Long-term survival of skin allografts induced by donor splenocytes and anti-CD154 antibody in thymectomized mice requires CD4(+) T cells, interferon-gamma, and CTLA4. *J Clin Invest*. 1998;101(11):2446–2455.
30. Feng G, et al. Exogenous IFN-gamma ex vivo shapes the alloreactive T-cell repertoire by inhibition of Th17 responses and generation of functional Foxp3+ regulatory T cells. *Eur J Immunol*. 2008;38(9):2512–2527.
31. Degauque N, et al. Immunostimulatory Tim-1-specific antibody deprograms Tregs and prevents transplant tolerance in mice. *J Clin Invest*. 2008; 118(2):735–741.
32. Rodriguez-Manzanet R, et al. TIM-4 expressed on APCs induces T cell expansion and survival. *J Immunol*. 2008;180(7):4706–4713.
33. Warren JR, Lalwani ND, Reddy JK. Phthalate esters as peroxisome proliferator carcinogens. *Environ Health Perspect*. 1982;45:35–40.
34. Brown JM, et al. The coincidence of myocardial reperfusion injury and hydrogen peroxide production in the isolated rat heart. *Surgery*. 1989;105(4):496–501.
35. Park D, Hochreiter-Hufford A, Ravichandran KS. The phosphatidylserine receptor TIM-4 does not mediate direct signaling. *Curr Biol*. 2009; 19(4):346–351.
36. Jones ND, et al. Differential susceptibility of heart, skin, and islet allografts to T cell-mediated rejection. *J Immunol*. 2001;166(4):2824–2830.
37. Li Y, Li XC, Zheng XX, Wells AD, Turka LA, Strom TB. Blocking both signal 1 and signal 2 of T-cell activation prevents apoptosis of alloreactive T cells and induction of peripheral allograft tolerance. *Nat Med*. 1999;5(11):1298–1302.
38. Schmelzle M, et al. CD39 modulates hematopoietic stem cell recruitment and promotes liver regeneration in mice and humans after partial hepatectomy. *Ann Surg*. 2013;257(4):693–701.
39. Saldanha-Araujo F, et al. Mesenchymal stromal cells up-regulate CD39 and increase adenosine production to suppress activated T-lymphocytes. *Stem Cell Res*. 2011;7(1):66–74.
40. Soriano P. Generalized lacZ expression with the ROSA26 Cre reporter strain. *Nat Genet*. 1999; 21(1):70–71.
41. Yeung MY, et al. Interruption of dendritic cell-mediated TIM-4 signaling induces regulatory T cells and promotes skin allograft survival. *J Immunol*. 2013;191(8):4447–4455.
42. Ueno T, et al. The emerging role of T cell Ig mucin 1 in alloimmune responses in an experimental mouse transplant model. *J Clin Invest*. 2008;118(2):742–751.
43. Kuchroo V, Umetsu D, DeKruyff R, Freeman G. The TIM gene family: emerging roles in immunity and disease. *Nat Rev Immunol*. 2003; 3(6):454–462.
44. Thornley TB, et al. Allograft rejection is restrained by short-lived TIM-3+PD-1+Foxp3+ Tregs. *J Clin Invest*. 2012;122(7):2395–2404.
45. Murphy SP, Porrett PM, Turka LA. Innate immunity in transplant tolerance and rejection. *Immunol Rev*. 2011;241(1):39–48.
46. Berney T, Secchi A. Rapamycin in islet transplantation: friend or foe? *Transpl Int*. 2009;22(2):153–161.
47. Liu W, Xiao X, Demirci G, Madsen J, Li XC. Innate NK cells and macrophages recognize and reject allogeneic nonself in vivo via different mechanisms. *J Immunol*. 2012;188(6):2703–2711.
48. Riquelme P, Geissler EK, Hutchinson JA. Alternative approaches to myeloid suppressor cell therapy in transplantation: comparing regulatory macrophages to tolerogenic DCs and MDSCs. *Transplant Res*. 2012;1(1):17.
49. Abe Y, et al. TIM-4 has dual function in the induction and effector phases of murine arthritis. *J Immunol*. 2013;191(9):4562–4572.
50. Lyszkiewicz M, et al. SIGN-R1+MHC II+ cells of the splenic marginal zone — a novel type of resident dendritic cells. *J Leukoc Biol*. 2011;89(4):607–622.
51. Rodriguez-Manzanet R, et al. T and B cell hyperactivity and autoimmunity associated with niche-specific defects in apoptotic body clearance in TIM-4-deficient mice. *Proc Natl Acad Sci U S A*. 2010;107(19):8706–8711.
52. Gaspari AA, Katz SI. Contact hypersensitivity. *Curr Protoc Immunol Chapter*. 2001; Chapter 4:Unit 4 2.
53. Strom TB, Tilney NL, Paradysz JM, Bancewicz J, Carpenter CB. Cellular components of allograft rejection: identity, specificity, and cytotoxic function of cells infiltrating acutely rejecting allografts. *J Immunol*. 1977;118(6):2020–2026.